Are pet clinical trials ready for prime time? *p. 638*

The sense (and antisense) of ALS therapy *pp. 647 & 708*

Keeping families in their homes *p. 694*

Science

$15
12 AUGUST 2016
sciencemag.org

AAAS

LONG IN THE TOOTH

400-year-old sharks in Arctic waters *p. 702*

dissociation of this excited state, producing radicals, or by the formation of a diol radical after reaction of an excited-state fatty acid with an adjacent molecule.

Because fatty acid–covered surfaces are ubiquitous, the photochemical production of gas-phase unsaturated and functionalized compounds will affect the local oxidative capacity of the atmosphere and will lead to secondary aerosol formation. This interfacial photochemistry may exert a very large impact, especially if in general the mere presence of a surface layer of a carboxylic acid can trigger this interfacial photochemistry at ocean surfaces, cloud droplets, and the surface of evanescent aerosol particles.

REFERENCES AND NOTES

1. C. George, M. Ammann, B. D'Anna, D. J. Donaldson, S. A. Nizkorodov, *Chem. Rev.* **115**, 4218–4258 (2015).
2. A. M. Baergen, D. J. Donaldson, *Environ. Sci. Technol.* **47**, 815–820 (2013).
3. Y. Dupart *et al.*, *Proc. Natl. Acad. Sci. U.S.A.* **109**, 20842–20847 (2012).
4. C. Zhu, B. Xiang, L. Zhu, R. Cole, *Chem. Phys. Lett.* **458**, 373–377 (2008).
5. S. Enami, M. R. Hoffmann, A. J. Colussi, *J. Phys. Chem. Lett.* **6**, 527–534 (2015).
6. M. T. C. Martins-Costa, J. M. Anglada, J. S. Francisco, M. F. Ruiz-Lopez, *J. Am. Chem. Soc.* **134**, 11821–11827 (2012).
7. M. T. C. Martins-Costa, F. F. García-Prieto, M. F. Ruiz-López, *Org. Biomol. Chem.* **13**, 1673–1679 (2015).
8. K. Mozgawa, B. Mennucci, L. Frediani, *J. Phys. Chem. C* **118**, 4715–4725 (2014).
9. R. Vácha, P. Slavíček, M. Mucha, B. J. Finlayson-Pitts, P. Jungwirth, *J. Phys. Chem. A* **108**, 11573–11579 (2004).
10. E. C. Griffith, R. J. Rapf, R. K. Shoemaker, B. K. Carpenter, V. Vaida, *J. Am. Chem. Soc.* **136**, 3784–3787 (2014).
11. R. Ciuraru *et al.*, *Environ. Sci. Technol.* **49**, 13199–13205 (2015).
12. R. Ciuraru *et al.*, *Sci. Rep.* **5**, 12741 (2015).
13. H. Fu *et al.*, *J. Am. Chem. Soc.* **137**, 8348–8351 (2015).
14. J. D. Coyle, *Chem. Rev.* **78**, 97–123 (1978).
15. L. R. Caswell, M. F. Howard, T. M. Onisto, *J. Org. Chem.* **41**, 3312–3316 (1976).
16. J. G. Calvert, J. N. Pitts, *Photochemistry* (Wiley, 1966).
17. S. Rossignol *et al.*, *Environ. Sci. Technol.* **48**, 3218–3227 (2014).
18. A. F. Parsons, *An Introduction to Free Radical Chemistry* (Blackwell Science, 2000).
19. J. M. C. Plane *et al.*, "Photochemistry in the sea-surface micorlayer" in *The Sea Surface and Global Change*, P. S. Liss, R. A. Duce, Eds. (Cambridge Univ. Press, 1997), pp. 71–93.
20. J. R. Kanicky, A. F. Poniatowski, N. R. Mehta, D. O. Shah, *Langmuir* **16**, 172–177 (2000).

ACKNOWLEDGMENTS

This study was supported by the European Research Council (ERC) under the European Union's Seventh Framework Program (FP/2007-2013)/ERC Grant Agreement 290852–AIRSEA. D.J.D. acknowledges ongoing support from the Natural Sciences and Engineering Research Council of Canada. The authors are grateful to P. Mascunan and N. Cristin for the ICP-MS analysis and N. Charbonnel and S. Perrier for the technical support provided by IRCELYON. All the data presented here can be downloaded from the supplementary materials.

SUPPLEMENTARY MATERIALS

www.sciencemag.org/content/353/6300/699/suppl/DC1
Materials and Methods
Figs. S1 to S6
Tables S1 to S3
References (*21*–*26*)
Database S1

29 January 2016; accepted 23 June 2016
10.1126/science.aaf3617

LIFE HISTORY

Eye lens radiocarbon reveals centuries of longevity in the Greenland shark (*Somniosus microcephalus*)

Julius Nielsen,[1,2,3,4]* Rasmus B. Hedeholm,[2] Jan Heinemeier,[5] Peter G. Bushnell,[6] Jørgen S. Christiansen,[4] Jesper Olsen,[5] Christopher Bronk Ramsey,[7] Richard W. Brill,[8,9] Malene Simon,[10] Kirstine F. Steffensen,[1] John F. Steffensen[1]

The Greenland shark (*Somniosus microcephalus*), an iconic species of the Arctic Seas, grows slowly and reaches >500 centimeters (cm) in total length, suggesting a life span well beyond those of other vertebrates. Radiocarbon dating of eye lens nuclei from 28 female Greenland sharks (81 to 502 cm in total length) revealed a life span of at least 272 years. Only the smallest sharks (220 cm or less) showed signs of the radiocarbon bomb pulse, a time marker of the early 1960s. The age ranges of prebomb sharks (reported as midpoint and extent of the 95.4% probability range) revealed the age at sexual maturity to be at least 156 ± 22 years, and the largest animal (502 cm) to be 392 ± 120 years old. Our results show that the Greenland shark is the longest-lived vertebrate known, and they raise concerns about species conservation.

The Greenland shark (Squaliformes, *Somniosus microcephalus*) is widely distributed in the North Atlantic, with a vertical distribution ranging from the surface to at least 1816-m depth (*1*, *2*). Females outgrow males, and adults typically measure 400 to 500 cm, making this shark species the largest fish native to arctic waters. Because reported annual growth is ≤1 cm (*3*), their longevity is likely to be exceptional. In general, the biology of the Greenland shark is poorly understood, and longevity and age at first reproduction are completely unknown. The species is categorized as "Data Deficient" in the Norwegian Red List (*4*).

Conventional growth zone chronologies cannot be used to age Greenland sharks because of their lack of calcified tissues (*5*). To circumvent this problem, we estimated the age from a chronology obtained from eye lens nuclei by applying radiocarbon dating techniques. In vertebrates, the eye lens nucleus is composed of metabolically inert crystalline proteins, which in the center (i.e., the embryonic nucleus) is formed during prenatal development (*6*, *7*). This tissue retains proteins synthetized at approximately age 0: a unique feature of the eye lens that has been exploited for other difficult-to-age vertebrates (*6*, *8*, *9*).

Our shark chronology was constructed from measurements of isotopes in the eye lens nuclei from 28 female specimens (81 to 502 cm total length, table S1) collected during scientific surveys in Greenland during 2010–2013 (fig. S1) (see supplementary materials). We used radiocarbon (^{14}C) levels [reported as percent of modern carbon (pMC)] to estimate ages and stable isotopes, ^{13}C and ^{15}N (table S1), to evaluate the carbon source (supplementary materials). Depleted $\delta^{13}C$ and enriched $\delta^{15}N$ levels established that the embryonic nucleus radiocarbon source was of dietary origin and represents a high trophic level. In other words, isotope signatures are dictated by the diet of the shark's mother, not the sampled animals. We set the terminal date for our analyses to 2012, because samples were collected over a 3-year period. The chronology presumes that size and age are positively correlated.

Since the mid-1950s, bomb–produced radiocarbon from atmospheric tests of thermonuclear weapons has been assimilated in the marine environment, creating a distinct "bomb pulse" in carbon-based chronologies (*10*). The period of rapid radiocarbon increase is a well-established time stamp for age validation of marine animals (*11*–*14*). Radiocarbon chronologies of dietary origin (reflecting the food web) and chronologies reflecting dissolved inorganic radiocarbon of surface mixed and deeper waters, have shown that the timing of the bomb pulse onset (i.e., when

[1]Marine Biological Section, University of Copenhagen, Strandpromenaden 5, 3000 Helsingør, Denmark. [2]Greenland Institute of Natural Resources, Post Office Box 570, Kivioq 2, 3900 Nuuk, Greenland. [3]Den Blå Planet, National Aquarium Denmark, Jacob Fortlingsvej 1, 2770 Kastrup, Denmark. [4]Department of Arctic and Marine Biology, UiT The Arctic University of Norway, 9037 Tromsø, Norway. [5]Aarhus AMS Centre, Department of Physics and Astronomy, Aarhus University, Ny Munkegade 120, 8000 Aarhus, Denmark. [6]Department of Biological Sciences, Indiana University South Bend, 1700 Mishawaka Avenue, South Bend, IN, USA. [7]Oxford Radiocarbon Accelerator Unit, University of Oxford, Dyson Perrins Building, South Parks Road, Oxford OX1 3QY, UK. [8]National Oceanic and Atmospheric Administration, National Marine Fisheries Service, Northeast Fisheries Science Center, James J. Howard Marine Sciences Laboratory, 74 Magruder Road, Highlands, NJ 07732, USA. [9]Virginia Institute of Marine Science, Post Office Box 1346, Gloucester Point, VA 23062, USA. [10]Greenland Climate Research Centre, Greenland Institute of Natural Resources, Post Office Box 570, Kivioq 2, 3900 Nuuk, Greenland.
***Corresponding author. Email: julius.nielsen@bio.ku.dk**

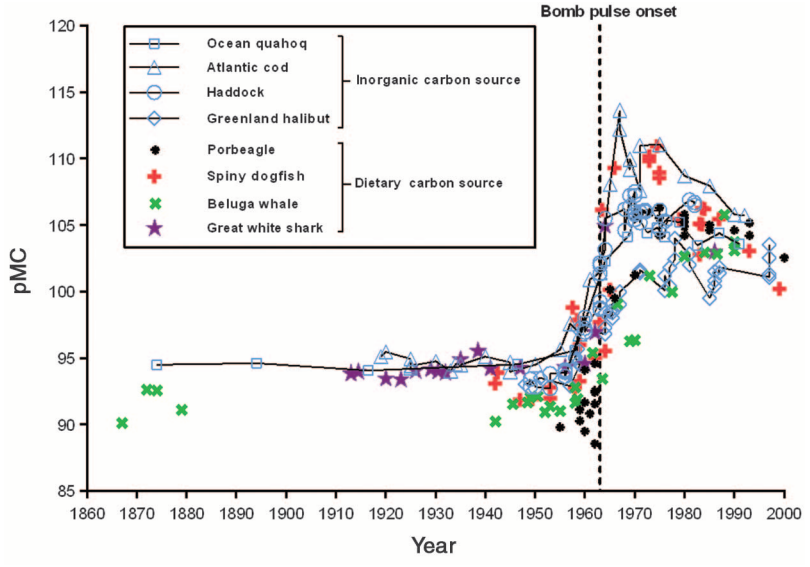

Fig. 1. Radiocarbon chronologies of the North Atlantic Ocean. Radiocarbon levels (pMC) of different origin (inorganic and dietary) over the past 150 years are shown. Open symbols (connected) reflect radiocarbon in marine carbonates (inorganic carbon source) of surface mixed and deeper waters (*26*, *36*–*38*). Solid symbols reflect radiocarbon in biogenic archives of dietary origin (*11*, *14*, *22*, *24*). The dashed vertical line indicates the bomb pulse onset in the marine food web in the early 1960s.

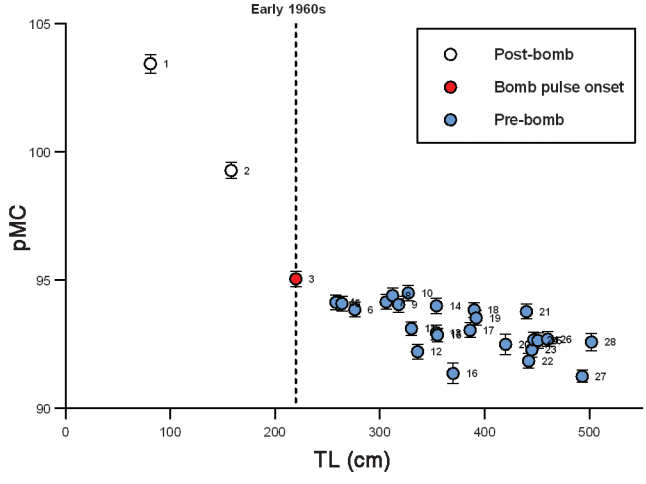

Fig. 2. Radiocarbon in eye lens nuclei of Greenland sharks. Radiocarbon levels (pMC ± SD, table S1) from 28 females plotted against total length (TL) are shown. Individual animals are identified by the numbers next to the symbols. Nos. 1 and 2 are of postbomb origin, and nos. 4 to 28 are of prebomb origin. We consider shark no. 3 to be from the early 1960s, which is the latest timing of the bomb pulse onset (dashed vertical line).

bomb-produced radiocarbon becomes detectable in a chronology) is synchronous within a few years and no later than early 1960s across the northern North Atlantic (Fig. 1).

Sexually mature females >400 cm have been caught across the Greenland continental shelf at depths between 132 and ~1200 m [(*15*, *16*) and table S1]. Their diet (*15*–*17*) and stable isotope signatures (*18*) (table S1) are comparable to those of other marine top predators such as the porbeagle (*Lamna nasus*), white shark (*Carcharodon carcharias*), spiny dogfish (*Squalus acanthias*), and beluga whale (*Delphinapterus leucas*) (*11*, *14*, *19*–*24*), for which the bomb pulse onset has been established (Fig. 1). We therefore consider the early 1960s as appropriate for the timing of the bomb pulse onset for the Greenland shark chronology as well.

The two smallest animals (nos. 1 and 2) had the highest radiocarbon levels (>99 pMC), implying that they were indeed affected by the bomb pulse (Fig. 2). However, given the variability of bomb pulse curves (Fig. 1), no exact age can be assigned to these animals other than that they were born later than the early 1960s. The third animal in the chronology (no. 3, 95.06 pMC), on the other hand, had a radiocarbon level slightly above those of the remaining sharks (nos. 4 to 28, pMC <95), placing its birth year close to the same time as the bomb pulse onset (i.e., early 1960s, Fig. 2). We therefore assign shark no. 3 (total length 220 cm) an age of ~50 years in 2012 and consider the remaining 25 larger animals to be of prebomb origin.

We estimated the age of prebomb sharks based on the Marine13 radiocarbon calibration curve (*25*), which evaluates carbon-based matter predating the bomb pulse that originates from surface mixed waters. The observed synchronicity of the bomb pulse onset (Fig. 1) supports the presumption that natural temporal changes of prebomb radiocarbon are imprinted in the marine food webs with negligible delay. We contend that the Marine13 curve can contribute to the assessment of the age of prebomb sharks despite the difficulties associated with (i) the low variation in the radiocarbon curve over the past 400 years (*25*); and (ii) that the degree of radiocarbon depletion in contemporaneous surface mixed waters (local reservoir age deviations, ΔR) differs between regions (*26*), meaning that the carbon source of the eye lens nucleus reflects food webs of potentially different ΔR levels. Consequently, radiocarbon levels of prebomb animals must be calibrated as a time series under a set of biological and environmental constraints.

We used OxCal (version 4.2) to do this calibration (*27*). The program uses Bayesian statistics to combine prior knowledge with calibrated age probability distributions to provide posterior age information (*28*, *29*). We constrained age ranges with presumptions about von Bertalanffy growth, size at birth, the age of animal no. 3 deduced from the bomb pulse onset (biological constraints), and plausible ΔR levels from the recent past (environmental constraint). This makes up a Bayesian model that is detailed in the supplementary materials.

Calibrations of single pMC measurements without biological constraints are shown as probability distributions of age with very wide ranges (light blue distributions, Fig. 3). When imposing the model, constrained and narrower age estimates are produced for each prebomb individual, shown as posterior probability distributions of age (dark blue distributions) in Fig. 3 and posterior calibrated age ranges at 95.4% (2σ) probability in table S2. OxCal also calculated agreement indices for each individual shark (A index) and for the calibration model (A_{model}). This allowed us to evaluate the consistency between modeled age ranges and Marine13, as well as the internal agreement between data points of the model (table S2) (*30*). To test the effect of the fixed age parameter (shark no. 3), a sensitivity analysis was made (supplementary materials and fig. S2), showing that the overall finding of extreme Greenland shark longevity is robust

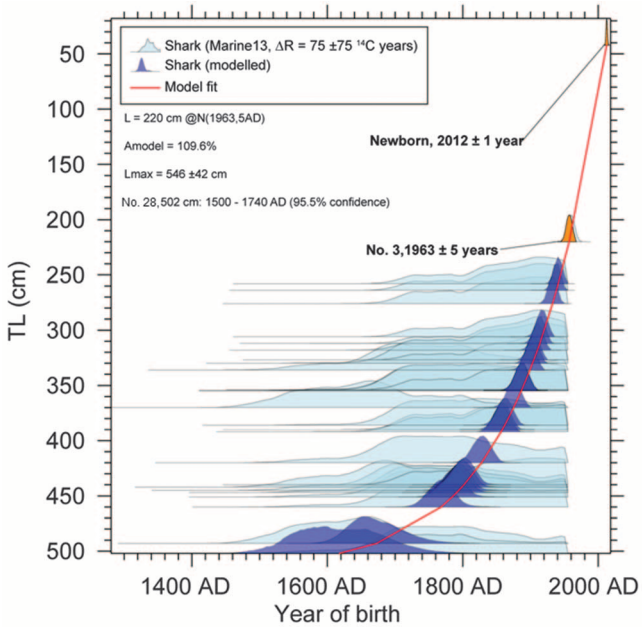

Fig. 3. Bayesian age ranges of prebomb sharks. The estimated year of birth against total length (TL) for prebomb sharks (nos. 4 to 28) is shown. Light blue shows the individual age probability distributions for each shark, and modeled posterior age probability distributions are shown in dark blue. Fixed age distributions (model input) of one newborn shark (42 cm, 2012 ± 1) and of shark no. 3 (220 cm, born in 1963 ± 5) are shown in orange. The red line is the model fit connecting the geometric mean for each posterior age probability distribution. (**Inset**) The model output; i.e., A_{model}, L_{max}, and range of birth year for shark no. 28. Also see the supplementary materials.

regardless of the exact timing of the bomb pulse onset (1958–1980).

The model estimated asymptotical total length to be 546 ± 42 cm (mean ± SD), a size matching the largest records for Greenland sharks (*2*), and the age estimates (reported as midpoint and extent of the 95.4% probability range) of the two largest Greenland sharks to be 335 ± 75 years (no. 27, 493 cm) and 392 ± 120 years (no. 28, 502 cm). Moreover, because females are reported to reach sexual maturity at lengths >400 cm (*15*), the corresponding age would be at least 156 ± 22 years (no. 19, 392 cm) (table S2). A_{model} was 109.6%, demonstrating that samples are in good internal agreement, implying that the age estimates are reliable.

The validity of our Greenland shark age estimates is supported by other lines of evidence. For instance, we found sharks <300 cm to be younger than 100 years (table S2). Such age estimates are indirectly corroborated by their depleted $\delta^{13}C$ levels (table S1), possibly reflecting the Suess effect, another chemical time mark triggered by emissions of fossil fuels, imprinted in marine food webs since the early 20th century (*31*, *32*). In addition, high levels of accumulated anthropogenic contaminants may suggest that ~300-cm females are older than 50 years (*33*). Taken together, these findings seem to corroborate an estimated life span of at least 272 years for Greenland sharks attaining more than 500 cm in length.

Our results demonstrate that the Greenland shark is among the longest-lived vertebrate species, surpassing even the bowhead whale (*Balaena mysticetus*, estimated longevity of 211 years) (*9*). The life expectancy of the Greenland shark is exceeded only by that of the ocean quahog (*Arctica islandica*, 507 years) (*34*). Our estimates strongly suggest a precautionary approach to the conservation of the Greenland shark, because they are common bycatch in arctic and subarctic groundfish fisheries and have been subjected to several recent commercial exploitation initiatives (*35*).

REFERENCES AND NOTES

1. H. B. Bigelow, W. C. Schroeder, in *Fishes of the Western North Atlantic*, A. E. Parr, Ed. (Yale University, New Haven, CT, 1948), pp. 516–523.
2. S. E. Campana, A. T. Fisk, A. P. Klimley, *Deep Sea Res. Part II Top. Stud. Oceanogr.* **115**, 109–115 (2015).
3. P. M. Hansen, *International Commission for the Northwest Atlantic Fisheries Special Publication* **4**, 172–175 (1963).
4. S. Henriksen, O. Hilmo, Eds., *Norsk Rødliste for Arter* (Artsdatabanken, Norge, 2015).
5. P. M. Kyne, C. A. Simpendorfer, Adaptive physiology and conservation, in *Sharks and Their Relatives*, J. C. Carrier, J. A. Musick, M. R. Heithaus, Eds. (CRC Press, 2010), pp. 37–71.
6. N. Lynnerup, H. Kjeldsen, S. Heegaard, C. Jacobsen, J. Heinemeier, *PLOS ONE* **3**, e1529 (2008).
7. S. Bassnett, Y. Shi, G. F. J. M. Vrensen, *Philos. Trans. R. Soc. London Ser. B* **366**, 1250–1264 (2011).
8. J. L. Bada, C. D. Vrolijk, S. Brown, E. R. M. Druffel, R. E. M. Hedges, *Geophys. Res. Lett.* **14**, 1065–1067 (1987).
9. J. C. George *et al.*, *Can. J. Zool.* **77**, 571–580 (1999).
10. H. De Vries, *Science* **128**, 250–251 (1958).
11. S. E. Campana, L. J. Natanson, S. Myklevoll, *Can. J. Fish. Aquat. Sci.* **59**, 450–455 (2002).
12. J. M. Kalish, *Earth Planet. Sci. Lett.* **114**, 549–554 (1993).
13. M. P. Francis, S. E. Campana, C. M. Jones, *Mar. Freshw. Res.* **58**, 10–23 (2007).
14. L. L. Hamady, L. J. Natanson, G. B. Skomal, S. R. Thorrold, *PLOS ONE* **9**, e84006 (2014).
15. K. Yano, J. D. Stevens, L. J. V. Compagno, *J. Fish Biol.* **70**, 374–390 (2007).
16. J. Nielsen, R. B. Hedeholm, M. Simon, J. F. Steffensen, *Polar Biol.* **37**, 37–46 (2014).
17. B. C. McMeans, J. Svavarsson, S. Dennard, A. T. Fisk, *Can. J. Fish. Aquat. Sci.* **67**, 1428–1438 (2010).
18. J. H. Hansen, R. B. Hedeholm, K. Sünksen, J. T. Christensen, P. Grønkjær, *Mar. Ecol. Prog. Ser.* **467**, 47–59 (2012).
19. L. J. V. Compagno, Ed., *FAO Species Catalogue. Vol. 4: Sharks of the World. An Annoted and Illustrated Catalogue of the Shark Species Known to Date. Part 1. Haxanchiformes to Lamniformes* (FAO Fisheries Synopsis, Food and Agriculture Organization of the United Nations, ed. 4, 1984).
20. M. P. Heide-Jørgensen, J. Teilman, *Biosci* **39**, 195–212 (1994).
21. W. N. Joyce *et al.*, *ICES J. Mar. Sci.* **59**, 1263–1269 (2002).
22. S. E. Campana, C. Jones, G. A. McFarlane, S. Myklevoll, *Environ. Biol. Fishes* **77**, 327–336 (2006).
23. J. A. Estrada, A. N. Rice, L. J. Natanson, G. B. Skomal, *Ecology* **87**, 829–834 (2006).
24. R. E. A. Stewart, S. E. Campana, C. M. Jones, B. E. Stewart, *Can. J. Zool.* **84**, 1840–1852 (2006).
25. P. J. Reimer *et al.*, *Radiocarbon* **55**, 1869–1887 (2013).
26. J. D. Scourse *et al.*, *Radiocarbon* **54**, 165–186 (2012).
27. C. Bronk Ramsey, *Radiocarbon* **37**, 425–430 (1995).
28. C. Bronk Ramsey, *Quat. Sci. Rev.* **27**, 42–60 (2008).
29. C. Bronk Ramsey, S. Lee, *Radiocarbon* **55**, 720–730 (2013).
30. C. Bronk Ramsey, *Radiocarbon* **51**, 1023–1045 (2009).
31. J. T. Christensen, K. Richardson, *Mar. Ecol. Prog. Ser.* **368**, 1–8 (2008).
32. P. G. Butler *et al.*, *Earth Planet. Sci. Lett.* **279**, 230–241 (2009).
33. A. T. Fisk, S. A. Tittlemier, J. L. Pranschke, R. J. Norstrom, *Ecology* **83**, 2162–2172 (2002).
34. P. G. Butler, A. D. Wanamaker Jr., J. D. Scourse, C. A. Richardson, D. J. Reynolds, *Palaeogeogr. Palaeocl.* **373**, 141–151 (2013).
35. R. B. Stouby, *Eksportkroner for Skidtfisk* (Eksportrådet: The Trade Council, Danish Ministry of Foreign Affairs 2, Copenhagen, Denmark, 2011).
36. S. E. Campana, *Mar. Ecol. Prog. Ser.* **150**, 49–56 (1997).
37. J. M. Kalish, R. Nydal, K. H. Nedreaas, G. S. Burr, G. L. Eine, *Radiocarbon* **43**, 843–855 (2001).
38. M. A. Treble, S. E. Campana, R. J. Wastle, C. N. Jones, J. Boje, *Can. J. Sci. Aquat. Sci.* **65**, 1047–1059 (2008).

ACKNOWLEDGMENTS

We are grateful for the contributions from M. B. Backe throughout the manuscript. We thank the Commission of Scientific Investigations in Greenland (KVUG), Save Our Seas Foundation, National Geographic Foundation, Carlsberg Foundation, Danish Centre for Marine Research, Den Blå Planet–National Aquarium of Denmark, Greenland Institute of Natural Resources (GINR), and the Danish Council for Independent Research for financial support. We thank GINR, the University of Copenhagen and the TUNU Programme (UIT, The Arctic University of Norway) for ship time. We are grateful for the collaboration with K.P. Lange. We thank the crews of the RV *Pâmiut*, RV *Dana*, RV *Helmer Hanssen*, RV *Sanna*, and RV *Porsild*. Three anonymous reviewers provided helpful comments and discussion that improved earlier versions of the manuscript.

SUPPLEMENTARY MATERIALS

www.sciencemag.org/content/353/6300/702/suppl/DC1
Material and Methods
Supplementary Text
Figs. S1 and S2
Tables S1 and S2
References (*39*–*50*)

29 December 2015; accepted 10 June 2016
10.1126/science.aaf1703

Eye lens radiocarbon reveals centuries of longevity in the Greenland shark (*Somniosus microcephalus*)

Julius Nielsen, Rasmus B. Hedeholm, Jan Heinemeier, Peter G. Bushnell, Jørgen S. Christiansen, Jesper Olsen, Christopher Bronk Ramsey, Richard W. Brill, Malene Simon, Kirstine F. Steffensen and John F. Steffensen (August 12, 2016)

Science **353** (6300), 702-704. [doi: 10.1126/science.aaf1703]

Editor's Summary

Science (print ISSN 0036-8075; online ISSN 1095-9203) is published weekly, except the last week in December, by the American Association for the Advancement of Science, 1200 New York Avenue NW, Washington, DC 20005.

www.sciencemag.org/content/353/6300/702/suppl/DC1

Supplementary Materials for

Eye lens radiocarbon reveals centuries of longevity in the Greenland shark (*Somniosus microcephalus*)

Julius Nielsen,* Rasmus B. Hedeholm, Jan Heinemeier, Peter G. Bushnell, Jørgen S. Christiansen, Jesper Olsen, Christopher Bronk Ramsey, Richard W. Brill, Malene Simon, Kirstine F. Steffensen, John F. Steffensen

*Corresponding author. Email: julius.nielsen@bio.ku.dk

Published 12 August 2016, *Science* **353**, 702 (2016)
DOI: 10.1126/science.aaf1703

This PDF file includes:

Materials and Methods

Sampling of sharks and eye lens nuclei

Analyzed sharks were caught from 2010-2013 as unintended bycatch during the Annual Fish Survey of Greenland Institute of Natural Resources, by the commercial fishing fleet and from scientific long lines. All sampling was carried out in accordance with laws and regulations and with authorization from the Government of Greenland (Ministry of Fisheries, Hunting & Agriculture, document number 565466 and 935119). Samples were taken from specimens with lethal injuries caused by conspecifics or fishing equipment. Sharks were euthanized immediately after capture by direct spinal cord transection. Total body length was measured and eye globes were removed and stored at -20^{o} C. The left eye lens was subsequently prepared at the Aarhus AMS Centre (Department of Physics and Astronomy, Aarhus University, Denmark) by isolating the embryonic eye lens nucleus under light microscopy from concentrically arranged layers of secondary fiber cells. A 4-5 mg subsample of the innermost part of the embryonic nucleus was used for isotopic analyses with Accelerator Mass Spectrometry (AMS) and Continuous-Flow Isotope Ratio Mass Spectrometry (CF-EA-IRMS).

Sample preparation and isotope measurements

Embryonic nucleus samples were converted to CO_2 by combustion at 950^{o} C in sealed evacuated quartz ampoules with CuO. A subsample of the resulting CO_2 gas was used for $\delta^{13}C$ Dual-Inlet analysis on an IsoPrime stable isotope ratio mass spectrometer to a precision of 0.02‰, while the rest was converted to graphite for AMS ^{14}C measurements (AMS Laboratory, Accium Biosciences, Seattle, WA, USA (*41*). The

results are reported according to international conventions (*42*) and ^{14}C content is given as percentage modern carbon (pMC) based on the measured $^{14}C/^{12}C$ ratio corrected for the natural isotopic fractionation by normalizing the $\delta^{13}C$ value to -25‰ VPDB (Vienna Pee Dee Belemnite; $\delta^{13}C$ calibration standard). The pMC unit is calculated as 100 * $F^{14}C$ (*43*) and reported as mean pMC ± SD. ^{14}C measurements are also presented as non-age corrected $\Delta^{14}C$ values where $\Delta^{14}C = (pMC/100 - 1) \times 1000$ ‰ (*44*). Stable isotopes, $\delta^{13}C$ and $\delta^{15}N$, were measured on eye lens nucleus samples weighed into tin cups at the Aarhus AMS Centre by continuous-flow isotope ratio mass spectrometry (Vario Cube elemental analyzer coupled to an IsoPrime stable isotope ratio mass spectrometer). All isotopic measurements are reported as mean ± SD. The instrument precision is determined by the standard deviation of ~16 measurements on the in house standard yielding ~0.2‰ for $\delta^{13}C$ and 0.2 – 0.5‰ for $\delta^{15}N$ for each analysis batch. The in house standard is a commercial gelatin which is calibrated against international IAEA standards. The statistical correlation between TL and $\delta^{13}C$, $\delta^{15}N$ and pre-bomb ^{14}C levels, were evaluated by Spearman's Rank Correlation Test.

Supplementary Text

Bayesian model design

The biological and environmental constraints of the Bayesian model are: 1) the largest shark with a bomb-induced ^{14}C signature is 49 ± 5 years old (which in the model input is fixed as mean ± SD), 2) length and age are positively correlated, where length increments decline asymptotically with age as expressed by a Von Bertalanffy growth

curve, 3) size at birth (i.e., age 0) is given by L_0 = 42 cm and 4) ΔR can vary according to a normal distribution of 75 ± 75 ^{14}C years (mean ± SD, N(75,75)).

By setting the largest shark with bomb-induced radiocarbon (no. 3 of 220 cm) to be 49 ± 5 years old (i.e. birth year 1963 ± 5, N(1963,5)) we introduce a time range that encompasses the earliest and latest detection of the bomb pulse rise in comparable marine food webs chronologies (Fig. 1) and also the first detection in metabolically active tissues of pelagic deep sea fauna (*45, 46*). This timing defines a sharp boundary for the successive time sequence of birth dates for the larger sharks which were also presumed to follow an exponential age-length expression:

$$L=L_{max} \cdot [1-\exp(-t/\tau)]$$

equivalent to a traditional Von Bertalanffy growth curve (*47*). Such growth patterns or derivate thereof have been demonstrated for multiple shark species (*48*). The sequence starts at the birth dates of the largest (presumed oldest) sharks and ends with a fictive newborn 0 years old shark of 42 cm fixed (i.e. year of birth 2012 ± 1). This size was chosen based on documented near term fetuses of 37 cm (*49*) and the smallest recorded free-swimming Greenland sharks of 41.8 cm TL (~42 cm) (*50*). The Bayesian statistics of the model assume a strict sequence of birth dates according to shark length. To incorporate the ΔR uncertainty, the model includes a ΔR value which is allowed to vary for individual sharks in the model according to a Gaussian distribution of around 75 ^{14}C years with a 1 sigma of 75 ^{14}C years. This ΔR range is representative for the resent past in

northern North Atlantic surface mixed waters (*27*). Results of the model output are illustrated in Fig. 3 as full posterior probability distributions for each shark. We present the age range estimates for each pre-bomb shark as 95.4 % (2 sigma) probability (table S2).

Bayesian model function

The Bayesian model was implemented in OxCal (version 4.2) (*28*-*30*, *32*). In the Bayesian analysis we define a uniform prior for the age of the longest shark t_l and for the time constant τ. Given the imposed constraints (see above), t_l and τ are the only independent parameters in the model. Given these two parameters, the length L_l of the longest shark, and the length at birth L_0, we can deduce the age t of any animal from its length L using the equation:

$$t = -\tau \ln\left(1 - \left(\frac{L - L_0}{L_l - L_0}\right)\left(1 - \exp\left(\frac{-t_l}{\tau}\right)\right)\right)$$

We sample over all possible values of the two independent parameters (t_l and τ) conditioned on the likelihood from the radiocarbon calibration applied to the radiocarbon measurements on the individual specimens. This gives us a marginal posterior distribution for τ and for the ages of each pre-bomb shark. We have used OxCal to implement this Bayesian model because it is already set up to calculate the likelihood distributions from radiocarbon calibration under such an exponential growth model (equation A44 in *29*). The code for implementing this model in OxCal is given below.

The agreement between model and data (A_{model}) are measured using the agreement indices which are a measure of the overlap between the un-modeled and modeled probability distributions provided by Oxcal (*51*). Generally A_{model} below 60% are considered as poor agreement.

Model priors and likelihoods

Parameter	Explanation
τ	Exponential time-constant for Von Bertalanffy growth curve
t_0	Collection date
t_1	Birth date of longest shark with bomb ^{14}C
t_i	Birth date of shark i, $1 < i < N$
t_N	Birth date of longest shark
d_i	Marine reservoir offset for shark i, $1 < i \leq N$
L_0	The length of sharks at birth (set at 42cm)
L_i	The length of shark i, $1 \leq i \leq N$
$r(t)$	Global marine radiocarbon calibration curve (GMRCC)
$s(t)$	Standard uncertainty in GMRCC
r_i	Radiocarbon date for shark i, $1 < i \leq N$
s_i	Standard uncertainty in radiocarbon date for shark i

The prior for the birth date of the oldest shark is uniform:

$$t_N \sim U(-\infty, t_0)$$

From this parameter the date of birth of all the other sharks can be estimated:

$$t_i = t_0 - \tau \cdot ln\left(1 - \frac{L_i - L_0}{L_N - L_0}\right) \cdot \left(1 - exp\left(-\frac{t_i}{\tau}\right)\right)$$

We define a uniform prior for τ:

$$\tau \sim U(0, \infty)$$

The local marine reservoir for each shark is independent and given a normal prior:

$$d_i = N(75, 75^2)$$

Given this and the marine calibration curve the likelihood from radiocarbon calibration is:

$$p(\theta|t_i) = \frac{1}{\sqrt{s_i^2 + s^2(t_i)}} exp\left(-\frac{\left(r_i - d_i - r(t_i)\right)^2}{2\left(s_i^2 + s^2(t_i)\right)}\right)$$

where Θ is the set of variable parameters. This applied to all the sharks $(1 < \boldsymbol{i} \leq N)$ except for the youngest shark which has been given a likelihood:

$$p(\theta|t_i) \propto N(AD(1963), 5^2)$$

The collection date is given a prior of:

$$t_0 \propto N(AD(2012), 1^2)$$

The informative independent variables in the model are τ and t_N. The only other independent variables are the marine reservoir offsets for the sharks d_i. MCMC is used to sample over the parameter space defined by $\{\tau, t_N, d_i\}$ using the priors and likelihoods defined above.

Model sensitivity test

Because we cannot verify the exact timing of the bomb pulse onset in the Greenland shark chronology, four additional model runs (scenarios) were conducted to test the model sensitivity of the birth year assigned to the shark with fixed age (no. 3, 220 cm, 49 ± 5 years). The four alternative scenarios are:

- Scenario 1: Shark no. 3 (length of 220 cm) is assumed a birth year of 1975, N(1975AD,5), corresponding to an age of 37 ± 5 years.
- Scenario 2: Shark no. 4 (length of 258 cm) is assumed a birth year of 1963, N(1963AD,5), corresponding to an age of 49 ± 5 years. In this scenario shark no. 3 is excluded from the model.

- Scenario 3: Shark no. 4 (length of 258 cm) is assumed a birth year of 1975, N(1975AD,5), corresponding to an age of 37 ± 5 years. In this scenario shark no. 3 is excluded from the model.
- Scenario 4: Shark no. 3 (length of 220 cm) is assumed a uniform prior birth year distribution between 1963 and 2012, U(1963AD,2012AD).

For the model to run these tests adequately the smallest seven sharks (shark nos. 3-10) are assumed to have an uniform prior age distribution, U(1700AD,1980AD). Studies from the Pacific Ocean show that all tissue samples from abyssopelagic and abyssobenthic fishes contained bomb-induced radiocarbon of dietary origin in the 1970s (*45, 46, 52*). Therefore, we contend that these alternative scenarios represent the most conservative estimates for the timing of the bomb pulse onset in the context of calibrating the Greenland shark chronology.

Model outputs are shown in Fig. S2. It is evident from all scenarios that the estimated age of shark no. 28 and asymptotic length (L_{max}) are robust to changes in fixed age of the youngest sharks. In all four scenarios the A_{model}-values were below 60% (indicating poor agreement between data and model assumptions), and well below that of the model presented in Fig. 3 (A_{model} = 109.6%). Interestingly, scenario 4, where the birth age of shark no. 3 was assigned a weak prior age probability distribution, U(1963AD,2012AD), produced a model output with the highest A_{model} (56 %) and is also most similar to the model presented in Fig. 3. This supports our contention, that the age of shark no. 3 being

~50 years is a valid estimate and hence that the fixed input of birth years between 1958-1968 for this shark in the model presented in Fig. 3 is appropriate.

Oxcal model code

```
Plot()
{
 Curve("Marine13", "marine13.14c");
 U_Sequence("Age_vs_Length")
 {
  Tau_Boundary("Tau")
  {
   color="green";
  };
  Delta_R("GS65DR",75, 75);
  R_Date("10 (GS65, 502 cm)",617,30)
  {
   z=502;
   color="blue";
  };
  Delta_R("GS67DR",75, 75);
  R_Date("16 (GS67 B, 493 cm)",736,21)
  {
   z=493;
   color="blue";
  };
  Delta_R("GS42DR",75, 75);
  R_Date("10, GS42 (460 cm)",608,25)
  {
   z=460;
   color="blue";
  };
  Delta_R("GS64DR",75, 75);
  R_Date("19 (GS64 B, 451 cm)",612,27)
  {
   z=451;
   color="blue";
  };
  Delta_R("GS2DR",75, 75);
  R_Date("15, GS2 (447 cm)",611,25)
  {
   z=447;
   color="blue";
  };
```

```
Delta_R("GS53DR",75, 75);
R_Date("06 (GS53, 445 cm)",645,27)
{
 z=445;
 color="blue";
};
Delta_R("GS5DR",75, 75);
R_Date("09, GS5 (442 cm)",682,25)
{
 z=442;
 color="blue";
};
Delta_R("GS80DR",75, 75);
R_Date("12 (GS80, 440 cm)",516,25)
{
 z=440;
 color="blue";
};
Delta_R("GS4DR",75, 75);
R_Date("08, GS4 (420 cm)",627,35)
{
 z=420;
 color="blue";
};
Delta_R("GS59DR",75, 75);
R_Date("09 (GS59, 392 cm)",537,25)
{
 z=392;
 color="blue";
};
Delta_R("GS58DR",75, 75);
R_Date("04 (GS58, 390 cm)",510,25)
{
 z=390;
 color="blue";
};
Delta_R("GS14DR",75, 75);
R_Date("07, GS14 (386 cm)",578,25)
{
 z=386;
 color="blue";
};
Date("Typical",U(1600,2000,5))
{
 z=375;
 color="green";
};
```

```
Delta_R("GS6DR",75, 75);
R_Date("13, GS6 (370 cm)",725,35)
{
 z=370;
 color="blue";
};
Delta_R("GS10DR",75, 75);
R_Date("06, GS10 (355 cm)",594,22)
{
 z=355;
 color="blue";
};
Delta_R("GS41DR",75, 75);
R_Date("14 (GS41, 354 cm)",586,25)
{
 z=354.5;
 color="blue";
};
Delta_R("GS55DR",75, 75);
R_Date("15 (GS55, 354 cm)",496,27)
{
 z=354;
 color="blue";
};
Delta_R("GS16DR",75, 75);
R_Date("05, GS16 (336 cm)",651,25)
{
 z=336;
 color="blue";
};
Delta_R("JFS2DR",75, 75);
R_Date("JFS2 (330 cm)",573,22)
{
 z=330;
 color="blue";
};
Delta_R("GS56",75, 75);
R_Date("08 (GS56, 327 cm)",454,26)
{
 z=327;
 color="blue";
};
Delta_R("GS81",75, 75);
R_Date("17 (GS81, 318 cm)",492,28)
{
 z=318;
 color="blue";
```

```
  };
  Delta_R("GS7",75, 75);
  R_Date("07 (GS7, 312 cm)",463,26)
  {
   z=312;
   color="blue";
  };
  Delta_R("GS12DR",75, 75);
  R_Date("04, GS12 (306 cm)",483,25)
  {
   z=306;
   color="blue";
  };
  Delta_R("GS19DR",75, 75);
  R_Date("11, GS19 (276 cm)",509,25)
  {
   z=276;
   color="blue";
  };
  Delta_R("GS13DR",75, 75);
  R_Date("03, GS13 (264 cm)",489,25)
  {
   z=264;
   color="blue";
  };
  Delta_R("GS3DR",75, 75);
  R_Date("02, GS3 (258 cm)",485,25)
  {
   z=258;
   color="blue";
  };
  Date("Shortest",N(AD(1963),5))
  {
   z=220;
   color="green";
  };
  Boundary("Newborn",N(AD(2012),1))
  {
   z=42;
   color="green";
  };
 };
 T=Newborn-Tau;
 TT=Newborn-Typical;
};
```

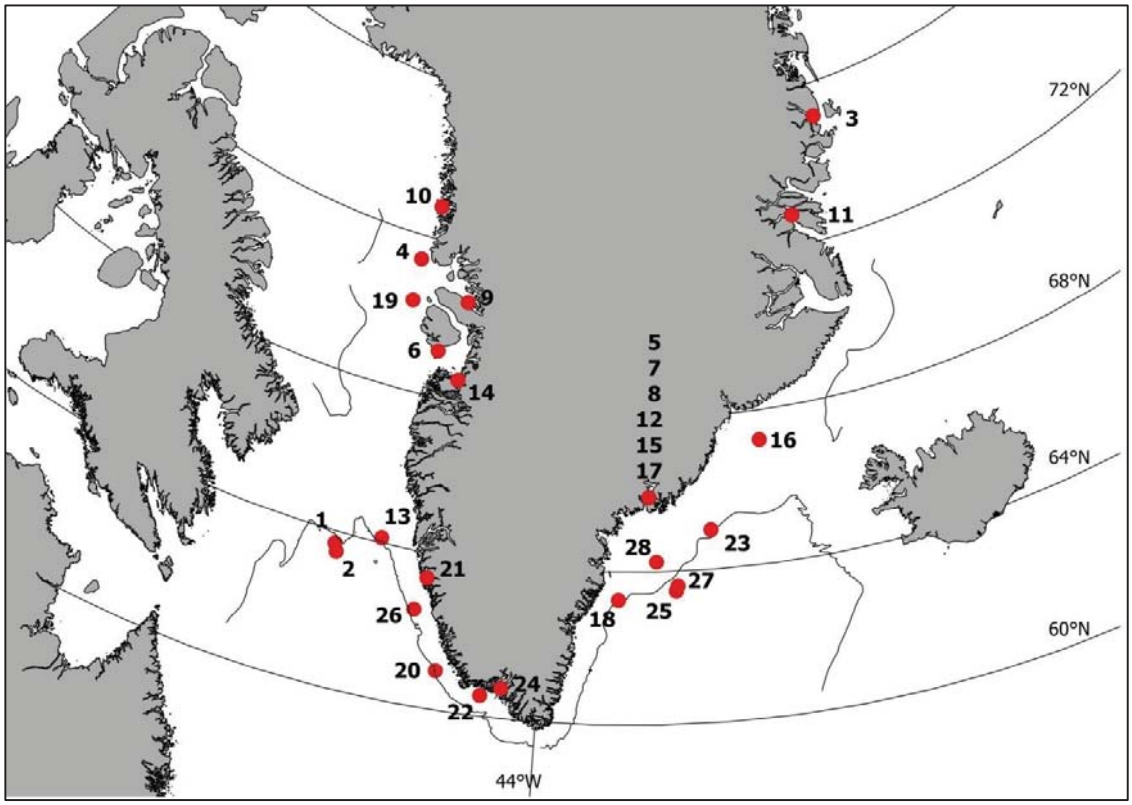

Fig. S1.

Capture positions of Greenland sharks around Greenland. Numbers next to the points identify the individual animals cf. Table S1.

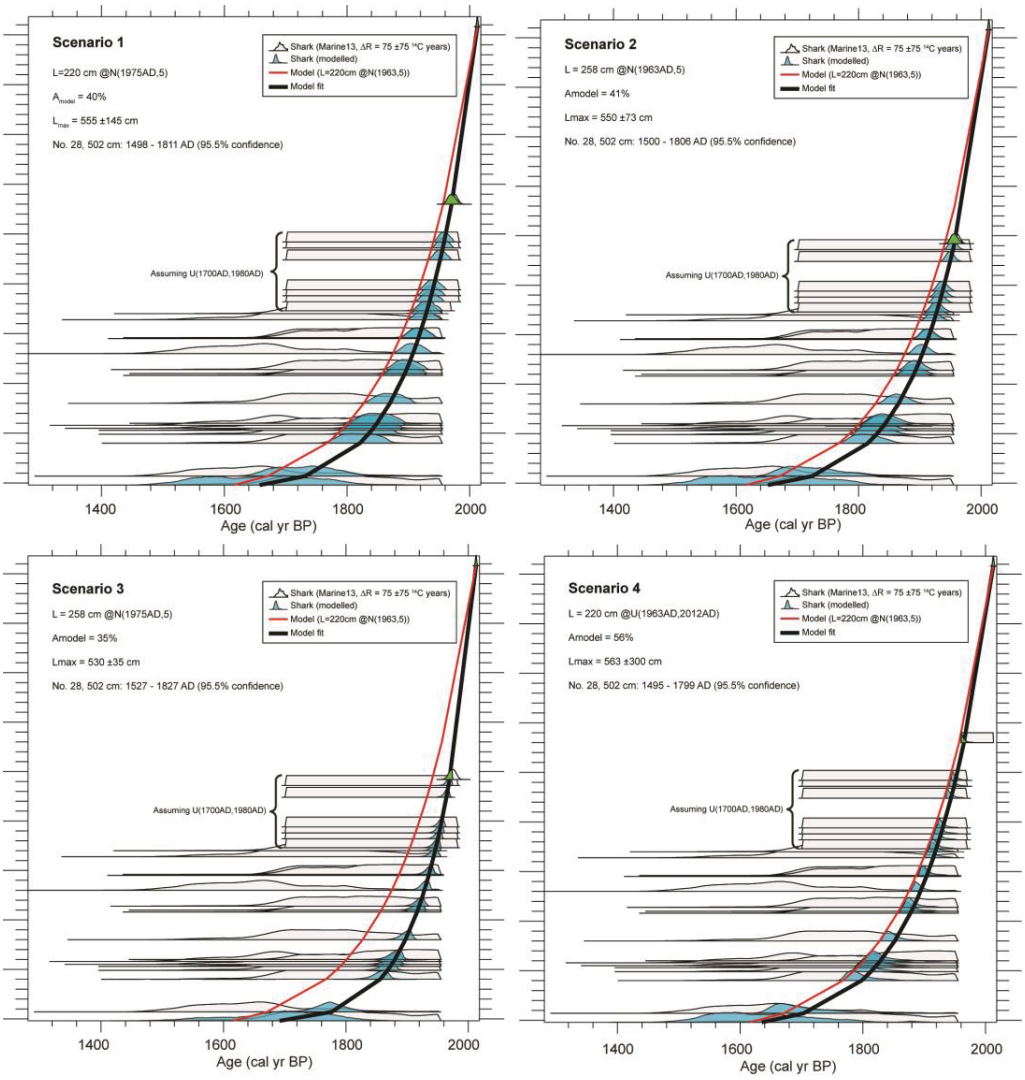

Fig. S2

Sensitivity analysis and Bayesian age ranges. Estimated year of birth against total length (TL, cm) from four different model scenarios. Scenario 1-3 are made with different fixed age of shark no. 3 (220 cm) or no. 4 (258 cm) with birth year either 1963 ± 5 years or 1975 ± 5 years, respectively. In scenario 4 the age of shark no. 3 is uniform in years 1963-2012. Light grey shows individual age probability distributions for each shark, whereas modelled posterior age probability distributions are shown in blue. Fixed distribution (model input) of one newborn shark (2012 ± 1) and the shark with the same age as the bomb pulse onset (37 ± 5 years or 49 ± 5 years) are shown in green. The black line is the model fit connecting the geometric mean for each posterior age probability distribution. The red line in each figure represents the similar line for the model presented in Fig. 3. Inserted, the model output i.e. A_{model}, L_{max}, and range of birth year for shark no. 28.

Table S1.

Overview of individual sharks and associated isotope levels. Total body length (TL) and capture depth for each shark with corresponding stable isotopes (reported as $\delta^{13}C$ and $\delta^{15}N$) and ^{14}C levels in pMC ($\Delta^{14}C$ are reported for conventional reasons). Sharks no. 1-3 had pMC levels >95 while the remaining individuals had pMC levels between 91.25-94.5 with a significant negative correlation between size and pMC (t=-4.18, df=23, P<0.001, cor=-0.66). $\delta^{13}C$ values ranged between -16.7 ‰ and -13.8 ‰ (mean ± SD= -14.9 ‰ ± 0.3, N=27) and $\delta^{15}N$ ranged between 12.0 ‰ and 17.6 ‰ (mean ± SD= 14.8 ± 0.2, N=27). $\delta^{13}C$ was positively correlated with TL (t=3.52, df=25, P<0.05, cor = 0.57) but not when only evaluated for sharks >300 cm (t=1.67, df=19, P=0.11, cor=0.36). There was no significant correlation between $\delta^{15}N$ and TL (t=0.49; df=25, P=0.63, cor =0.10). AAR-number refers to laboratory identification number at Aarhus AMS Centre, Aarhus University.

No	AAR-ID	TL (cm)	Depth (m)	$\delta^{13}C$ ± SD	$\delta^{15}N$ ± SD	$\Delta^{14}C$	pMC ± SD
1	19177	81	540	-15.9 ± 0.3	16.0 ± 0.3	34.4	103.44 ± 0.37
2	18075	158	1100	-15.5 ± 0.1	12.0 ± 0.1	-7.2	99.28 ± 0.32
3	19179	220	325	-16.2 ± 0.3	15.2 ± 0.2	-49.4	95.06 ± 0.30
4	18076,3	258	175	-15.3 ± 0.2	14.1 ± 0.2	-58.6	94.14 ± 0.29
5	18077	264	380	-15.1 ± 0.2	13.8 ± 0.2	-59.1	94.09 ± 0.29
6	18085	276	205	-15.2 ± 0.2	14.6 ± 0.2	-61.4	93.86 ± 0.29
7	18078	306	394	-15.0 ± 0.2	16.0 ± 0.2	-58.4	94.16 ± 0.29
8	19183	312	350	-14.0 ± 0.5	13.9 ± 0.4	-56.0	94.40 ± 0.30
9	19193	318	990	-16.7 ± 0.5	17.6 ± 0.4	-59.4	94.06 ± 0.32
10	19184	327	296	-15.4 ± 0.3	13.2 ± 0.4	-55.0	94.50 ± 0.30
11	14646	330	500	-	-	-68.8	93.12 ± 0.27
12	18079	336	596	-14.5 ± 0.2	13.5 ± 0.2	-77.8	92.22 ± 0.29
13	19190	354	492	-15.3 ± 0.3	13.5 ± 0.3	-70.4	92.96 ± 0.29
14	19191	354	407	-14.9 ± 0.3	14.0 ± 0.4	-59.9	94.01 ± 0.31
15	18080,3	355	454	-14.3 ± 0.2	15.5 ± 0.2	-71.3	92.87 ± 0.26
16	18087	370	555	-14.4 ± 0.2	14.8 ± 0.2	-86.3	91.37 ± 0.40
17	18081	386	567	-14.8 ± 0.2	15.2 ± 0.2	-69.4	93.06 ± 0.29
18	19180	390	507	-15.0 ± 0.3	17.6 ± 0.4	-61.5	93.85 ± 0.29
19	19185	391	500	-15.2 ± 0.5	14.7 ± 0.4	-64.7	93.53 ± 0.29
20	18082	420	178	-14.5 ± 0.2	16.9 ± 0.2	-75.0	92.50 ± 0.40
21	19188	440	602	-14.7 ± 0.3	13.2 ± 0.3	-62.2	93.78 ± 0.29
22	18083	442	132	-14.7 ± 0.2	14.3 ± 0.2	-81.4	91.86 ± 0.29
23	19182	445	210	-14.4 ± 0.3	15.7 ± 0.3	-77.1	92.29 ± 0.31
24	18089	447	308	-14.6 ± 0.2	15.3 ± 0.2	-73.2	92.68 ± 0.29
25	19195	451	900	-15.7 ± 0.3	14.2 ± 0.3	-73.4	92.66 ± 0.31
26	18084,3	460	133	-14.6 ± 0.2	12.7 ± 0.2	-72.9	92.71 ± 0.29
27	19192	493	900	-13.8 ± 0.3	16.0 ± 0.4	-87.5	91.25 ± 0.24
28	19186	502	900	-14.5 ± 0.3	14.7 ± 0.3	-74.0	92.60 ± 0.35

Table S2.

Modelled age estimates for pre-bomb sharks. For each shark length (TL), the associated posterior calibrated biological age ranges at 95.4% (2 sigma) probability (reported as mid-point value ± 1/2 range) are presented together with the associated A index as produced by the Bayesian model. A index values > 60% reflect a good level of consistency between modelled age ranges and Marine13. Three sharks had an A index value < 60%. Although it is not possible to isolate a single reason for this, it is likely to be a combination of variation in local reservoir age combined with deviations from the strict age and length assumption in the model.

No	TL (cm)	Age range (95.4 %)	A index (%)
4	258	71 ± 12	128.6
5	264	73 ± 14	130.2
6	276	80 ± 13	129.6
7	306	96 ± 15	139.4
8	312	99 ± 15	143.0
9	318	102 ± 15	136.4
10	327	108 ± 16	139.4
11	330	110 ± 18	99.6
12	336	113 ± 17	50.0
13	354	126 ± 19	123.5
14	354	126 ± 19	100.0
15	355	126 ± 19	96.0
16	370	137 ± 20	20.1
17	386	150 ± 22	111.8
18	390	155 ± 23	113.2
19	392	156 ± 22	116.9
20	420	185 ± 26	108.2
21	440	212 ± 31	71.9
22	442	215 ± 33	106.7
23	445	220 ± 33	125.7
24	447	223 ± 33	122.1
25	451	229 ± 33	122.7
26	460	245 ± 38	121.5
27	493	335 ± 75	120.0
28	502	392 ± 120	35.9

References and Notes

1. H. B. Bigelow, W. C. Schroeder, "*Sharks*" in *Fishes of the Western North Atlantic*, A. E. Parr, Ed. (Yale University, New Haven, CT, 1948), pp. 516–523.

2. S. E. Campana, A. T. Fisk, A. P. Klimley, Movements of Arctic and northwest Atlantic Greenland sharks (*Somniosus microcephalus*) monitored with archival satellite pop-up tags suggest long-range migrations. *Deep Sea Res. Part II Top. Stud. Oceanogr.* **115**, 109–115 (2015). doi:10.1016/j.dsr2.2013.11.001

3. P. M. Hansen, *International Commission for the Northwest Atlantic Fisheries Special Publication* **4**, 172–175 (1963).

4. S. Henriksen, O. Hilmo, Eds., *Norsk Rødliste for Arter* (Artsdatabanken, Norge, 2015).

5. P. M. Kyne, C. A. Simpendorfer, Adaptive physiology and conservation, in *Sharks and Their Relatives*, J. C. Carrier, J. A. Musick, M. R. Heithaus, Eds. (CRC Press, 2010), pp. 37–71.

6. N. Lynnerup, H. Kjeldsen, S. Heegaard, C. Jacobsen, J. Heinemeier, Radiocarbon dating of the human eye lens crystallines reveal proteins without carbon turnover throughout life. *PLOS ONE* **3**, e1529 (2008). doi:10.1371/journal.pone.0001529

7. S. Bassnett, Y. Shi, G. F. J. M. Vrensen, Biological glass: Structural determinants of eye lens transparency. *Philos. Trans. R. Soc. London Ser. B* **366**, 1250–1264 (2011). doi:10.1098/rstb.2010.0302

8. J. L. Bada, C. D. Vrolijk, S. Brown, E. R. M. Druffel, R. E. M. Hedges, Bomb radiocarbon in metabolically inert tissues from terrestrial and marine mammals. *Geophys. Res. Lett.* **14**, 1065–1067 (1987). doi:10.1029/GL014i010p01065

9. J. C. George, J. Bada, J. Zeh, L. Scott, S. E. Brown, T. O'Hara, R. Suydam, Age and growth estimates of bowhead whales (*Balaena mysticetus*) via aspartic acid racemization. *Can. J. Zool.* **77**, 571–580 (1999). doi:10.1139/cjz-77-4-571

10. H. De Vries, Atomic bomb effect: Variation of radiocarbon in plants, shells, and snails in the past 4 years. *Science* **128**, 250–251 (1958). Medline doi:10.1126/science.128.3318.250

11. S. E. Campana, L. J. Natanson, S. Myklevoll, Bomb dating and age determination of large pelagic sharks. *Can. J. Fish. Aquat. Sci.* **59**, 450–455 (2002). doi:10.1139/f02-027

12. J. M. Kalish, Pre- and post-bomb radiocarbon in fish otoliths. *Earth Planet. Sci. Lett.* **114**, 549–554 (1993). doi:10.1016/0012-821X(93)90082-K

13. M. P. Francis, S. E. Campana, C. M. Jones, Age under-estimation in New Zealand porbeagle sharks (*Lamna nasus*): Is there an upper limit to ages that can be determined from shark vertebrae? *Mar. Freshw. Res.* **58**, 10–23 (2007). doi:10.1071/MF06069

14. L. L. Hamady, L. J. Natanson, G. B. Skomal, S. R. Thorrold, Vertebral bomb radiocarbon suggests extreme longevity in white sharks. *PLOS ONE* **9**, e84006 (2014). doi:10.1371/journal.pone.0084006

15. K. Yano, J. D. Stevens, L. J. V. Compagno, Distribution, reproduction and feeding of the Greenland shark *Somniosus (Somniosus) microcephalus*, with notes on two other sleeper

sharks, *Somniosus (Somniosus) pacificus* and *Somniosus (Somniosus) antarcticus*. *J. Fish Biol.* **70**, 374–390 (2007). doi:10.1111/j.1095-8649.2007.01308.x

16. J. Nielsen, R. B. Hedeholm, M. Simon, J. F. Steffensen, Distribution and feeding ecology of the Greenland shark (*Somniosus microcephalus*) in Greenland waters. *Polar Biol.* **37**, 37–46 (2014). doi:10.1007/s00300-013-1408-3

17. B. C. McMeans, J. Svavarsson, S. Dennard, A. T. Fisk, Diet and resource use among Greenland sharks (*Somniosus microcephalus*) and teleosts sampled in Icelandic waters, using $\delta^{13}C$, $\delta^{15}N$, and mercury. *Can. J. Fish. Aquat. Sci.* **67**, 1428–1438 (2010). doi:10.1139/F10-072

18. J. H. Hansen, R. B. Hedeholm, K. Sünksen, J. T. Christensen, P. Grønkjær, Spatial variability of carbon ($\delta^{13}C$) and nitrogen ($\delta^{15}N$) stable isotope ratios in an Arctic marine food web. *Mar. Ecol. Prog. Ser.* **467**, 47–59 (2012). doi:10.3354/meps09945

19. L. J. V. Compagno, Ed., *FAO Species Catalogue. Vol. 4: Sharks of the World. An Annoted and Illustrated Catalogue of the Shark Species Known to Date. Part 1. Haxanchiformes to Lamniformes* (FAO Fisheries Synopsis, Food and Agriculture Organization of the United Nations, ed. 4, 1984).

20. M. P. Heide-Jørgensen, J. Teilman, *Biosci* **39**, 195–212 (1994).

21. W. N. Joyce, S. E. Campana, L. J. Natanson, N. E. Kohler, H. L. Pratt Jr., C. F. Jensen, Analysis of stomach contents of the porbeagle shark (*Lamna nasus* Bonnaterre) in the northwest Atlantic. *ICES J. Mar. Sci.* **59**, 1263–1269 (2002). doi:10.1006/jmsc.2002.1286

22. S. E. Campana, C. Jones, G. A. McFarlane, S. Myklevoll, Bomb dating and age validation using the spines of spiny dogfish (*Squalus acanthias*). *Environ. Biol. Fishes* **77**, 327–336 (2006). doi:10.1007/s10641-006-9107-3

23. J. A. Estrada, A. N. Rice, L. J. Natanson, G. B. Skomal, Use of isotopic analysis of vertebrae in reconstructing ontogenetic feeding ecology in white sharks. *Ecology* **87**, 829–834 (2006). Medline doi:10.1890/0012-9658(2006)87[829:UOIAOV]2.0.CO;2

24. R. E. A. Stewart, S. E. Campana, C. M. Jones, B. E. Stewart, Bomb radiocarbon dating calibrates beluga (*Delphinapterus leucas*) age estimates. *Can. J. Zool.* **84**, 1840–1852 (2006). doi:10.1139/z06-182

25. P. J. Reimer, E. Bard,, A. Bayliss, J. W. Beck, P. G. Blackwell, C. Bronk Ramsey, C. E. Buck, H. Cheng, R. L. Edwards, M. Friedrich, P. M. Grootes, T. P. Guilderson, H. Haflidason, I. Hajdas, C. Hatté, T. J. Heaton, D. L. Hoffman, A. G. Hogg, K. A. Hughen, K. F. Kaiser, B. Kromer, S. W. Manning, M. Niu, R. W. Reimer, D. A. Richards, E. M. Scott, J. R. Southon, R. A. Staff, C. S. M. Turney, J. van der Plicht, IntCal13 and Marine13 radiocarbon age calibration curves 0–50,000 years cal BP. *Radiocarbon* **55**, 1869–1887 (2013). doi:10.2458/azu_js_rc.55.16947

26. J. D. Scourse, A. Wanamaker Jr., C. Weidman, J. Heinemeier, P. Reimer, P. Butler, R. Witbaard, C. Richardson, The marine radiocarbon bomb pulse across the temperate North Atlantic: A compilation of $\Delta^{14}C$ time histories from *Arctica islandica* growth increments. *Radiocarbon* **54**, 165–186 (2012). doi:10.2458/azu_js_rc.v54i2.16026

27. C. Bronk Ramsey, *Radiocarbon* **37**, 425–430 (1995).

28. C. Bronk Ramsey, Deposition models for chronological records. *Quat. Sci. Rev.* **27**, 42–60 (2008). doi:10.1016/j.quascirev.2007.01.019

29. C. Bronk Ramsey, S. Lee, *Radiocarbon* **55**, 720–730 (2013).

30. C. Bronk Ramsey, *Radiocarbon* **51**, 1023–1045 (2009).

31. J. T. Christensen, K. Richardson, Stable isotope evidence of long-term changes in the North Sea food web structure. *Mar. Ecol. Prog. Ser.* **368**, 1–8 (2008). doi:10.3354/meps07635

32. P. G. Butler, J. D. Scourse, C. A. Richardson, A. D. Wanamaker Jr., C. L. Bryant, J. D. Bennell, Continuous marine radiocarbon reservoir calibration and the ^{13}C Suess effect in the Irish Sea: Results from the first multi-centennial shell-based marine master chronology. *Earth Planet. Sci. Lett.* **279**, 230–241 (2009). doi:10.1016/j.epsl.2008.12.043

33. A. T. Fisk, S. A. Tittlemier, J. L. Pranschke, R. J. Norstrom, Using anthropogenic contaminants and stable isotopes to assess the feeding ecology of Greenland sharks. *Ecology* **83**, 2162–2172 (2002). doi:10.1890/0012-9658(2002)083[2162:UACASI]2.0.CO;2

34. P. G. Butler, A. D. Wanamaker Jr., J. D. Scourse, C. A. Richardson, D. J. Reynolds, Variability of marine climate on the North Icelandic Shelf in a 1357-year proxy archive based on growth increments in the bivalve *Arctica islandica*. *Palaeogeogr. Palaeocl.* **373**, 141–151 (2013). doi:10.1016/j.palaeo.2012.01.016

35. R. B. Stouby, *Eksportkroner for Skidtfisk* (Eksportrådet: The Trade Council, Danish Ministry of Foreign Affairs 2, Copenhagen, Denmark, 2011).

36. S. E. Campana, Use of radiocarbon from nuclear fallout as a dated marker in the otoliths of haddock *Melanogrammus aeglefinus*. *Mar. Ecol. Prog. Ser.* **150**, 49–56 (1997). doi:10.3354/meps150049

37. J. M. Kalish, R. Nydal, K. H. Nedreaas, G. S. Burr, G. L. Eine, *Radiocarbon* **43**, 843–855 (2001).

38. M. A. Treble, S. E. Campana, R. J. Wastle, C. N. Jones, J. Boje, Growth analysis and age validation of a deepwater Arctic fish, the Greenland halibut (*Reinhardtius hippoglossoides*). *Can. J. Sci. Aquat. Sci.* **65**, 1047–1059 (2008). doi:10.1139/F08-030

39. U. Zoppi, J. Crye, Q. Song, A. Arjomand, *Radiocarbon* **49**, 173–182 (2007).

40. M. Stuiver, H. A. Polach, *Radiocarbon* **19**, 355–363 (1977).

41. P. J. Reimer, T. A. Brown, R. W. Reimer, *Radiocarbon* **46**, 1299–1304 (2004).

42. A. Mahadevan, An analysis of bomb radiocarbon trends in the Pacific. *Mar. Chem.* **73**, 273–290 (2001). doi:10.1016/S0304-4203(00)00113-4

43. P. M. Williams, J. A. McGowan, M. Stuiver, Body carbon-14 in deep sea organisms. *Nature* **227**, 375–376 (1970). Medline doi:10.1038/227375a0

44. P. M. Williams, E. R. M. Druffel, K. L. Smith Jr., Dietary carbon sources for deep-sea organisms as inferred from their organic radiocarbon activities. *Deep-Sea Res.* **34**, 253–266 (1987). doi:10.1016/0198-0149(87)90085-9

45. L. V. Bertalanffy, *Hum. Biol.* **10**, 181–213 (1938).

46. J. M. Hoenig, S. H. Gruber, *Elasmobranchs as Living Resources: Advances in the Biology, Ecology, Systematics and the Status of the Fisheries* (NOAA Technical Report 90, National Oceanic and Atmospheric Administration, Honolulu, HI, 1990).

47. E. Kofoed, *Report on Norwegian Fishery and Marine Investigations* **11**, 8–12 (1957).

48. E. I. Kukuev, I. A. Trunov, *J. Ichthyol.* **42**, 377–384 (2002).

49. C. Bronk Ramsey, *Radiocarbon* **51**, 337–360 (2009).

50. W. G. Pearcy, M. Stuiver, Vertical transport of carbon-14 into deep-sea food webs. *Deep-Sea Res.* **30**, 427–440 (1983). doi:10.1016/0198-0149(83)90076-6